water

MDPI

Article

Orographic Effects of Geomorphology on Precipitation in a Pluvial Basin of the Eastern Tibetan Plateau

Mei Yang [1,*] and Wenjiang Zhang [2]

[1] College of Water Resources Science and Engineering, Taiyuan University of Technology, Taiyuan 030024, China

[2] State Key Laboratory of Hydraulics and Mountain River, Sichuan University, Chengdu 610065, China; zhangwj@lreis.ac.cn

* Correspondence: yangmei@tyut.edu.cn; Tel.: +86-135-136-48762

Received: 18 December 2018; Accepted: 29 January 2019; Published: 31 January 2019

check for updates

Abstract: The eastern Tibetan Plateau is subjected to strong spatial variations in precipitation, but the underlying reasons are still not well understood due to sparse in-situ meteorological observations. In this study, streamflow observations were adopted to investigate the orographic controls on precipitation in the Qingyijiang (QYJ) Basin of the eastern Tibetan Plateau. The method of multi-year annual water balance was used to estimate the basin-level precipitation using in-situ streamflow and flux-based evapotranspiration. In addition, elevation transect was designed to examine the possible links between precipitation and geomorphology. The results showed the severe under-estimation of regional precipitation by weather sites (~1150 mm yr^{-1}) in the QYJ Basin, where the runoff depth was as high as ~1450 mm yr^{-1}. The water balance revealed a much higher level of precipitation (~2000 mm yr^{-1}) in the QYJ Basin, but precipitation in the two adjacent basins was contrastingly low (<1000 mm yr^{-1}). The spatial pattern of precipitation was well consistent with the local horn-mouth geomorphology, with more precipitation occurring in the geomorphologically converging and elevating region. Furthermore, within the the QYJ Basin, annual precipitation was larger in the sub-basins (>2200 mm) on or near the bottom of the horn-mouth geomorphology than the others (<1800 mm). With these results, we concluded that the high precipitation level in the QYJ Basin could be attributed to the combined converging and lifting effects of geomorphology on the westward atmospheric vapor. Therefore, flooding risk should be carefully accounted for in the basins with similar geomorphology in the eastern Tibetan Plateau.

Keywords: geomorphology; orographic effect; precipitation; runoff depth; Tibetan Plateau

1. Introduction

The Tibetan Plateau (TP) is the largest highland (~2.5 × 10^6 km^2) in the world with an elevation of over 4000 m above sea level [1], and the adjacent lowlands are mostly below 2000 m in elevation [2]. Under the combined influences of Asian Summer Monsoon (ASM) and Indian Ocean Monsoon (IOM), the mountains at the south and east TP boundaries intercept abundant water vapor, and thus produce a high level of runoff in the mountain areas [3–5]. Therefore, the TP is an important regional water source of many Asian major rivers, including the Mekong, Yangtze, Yellow, Indus, and Brahmaputra rivers [6].

Generally, precipitation in mountainous regions can be modulated by both local terrain characteristics and mesoscale geomorphology [7–12]. Complex orography is thought to control local precipitation patterns by determining the location and rate of upward air motion and triggering microphysical processes [13]. The height, slope, direction and combination of mountain chains are the major orographic properties influencing precipitation [14,15]. The flow blocking and splitting due to relief is found to significantly impact the intensity and distribution of orographic precipitation [14]. For example, the upslope ascent dominated and the precipitation intensity is proportionally related to the mountain height and wind speed in the low mountains. However, this relationship will not hold true in high mountains because the lifting effect is reduced by moisture lowering when air flow gets over the terrain peak. It is showed that the impact of orography also depends on the nature of the precipitation regime [16]. As the TP is over 2000 m above the adjacent regions, it has a distinct blocking effect on the vapor transporting to the plateau hinterland [10,17]. Therefore, orographic precipitation prevails in the mountainous areas of south and east TP [18].

Precipitation and runoff production in the southeast and east TP mountains show the pronounced spatial heterogeneity due to the orographic effect on atmospheric vapor transporting [5,19,20]. Many studies have focused on the vapor corridors of the Indian Ocean Monsoon entering the TP, such as at lower reaches of the Brahmaputra, Salween and Mekong [4,5,18,21,22]. The Indian Ocean is thought of as the major vapor source for the TP, which leads to the northwesterly decreasing trend in precipitation, i.e., varying from over 5000 mm to below 100 mm in the TP [1,5,23]. Therefore, a strong orographic effect results in the extremely high level of precipitation along the valley of lower Brahmaputra, such as at Cherrapunji where the largest annual precipitation on the earth (over 10,000 mm yr^{-1}) was recorded [18,21,22].

The vapor carried by the Asian Summer Monsoon westward from the Pacific is another important atmospheric water source for the TP [7,10,24]. However, vapor transporting from this source is relatively less studied partially due to the smaller moisture flux than that of the Indian Ocean Monsoon. The characteristics of orographic effect-related precipitation in mountainous areas of the eastern TP are still not well understood. In the eastern TP, the Qingyijiang (QYJ) is a typical river that runs through the plateau boundary (>4000 m) to an adjacent lowland region (i.e., the Sichuan Basin, ~500 m). The QYJ Basin has abundant precipitation and runoff much higher than adjacent basins, though these basins are all under the influences of ASM. Detailed understanding about the contrasting precipitation among these hydrological basins is limited by the scarcity of in-situ meteorological observations [7,12,17]. Streamflow records may provide the alternative material to represent precipitation for the basins subjected to strong orographic effects [25].

Satellite precipitation does hold a great potential for providing regional high-resolution precipitation information, but more evaluations are still needed on the feasibility of satellite precipitation products in mountainous regions such as the QYJ Basin. The calibration of satellite precipitation is highly dependent on necessary ground measurements of precipitation, so the current satellite products still have serious uncertainties in quantifying precipitation in the Tibetan mountains [26,27]. Therefore, satellite products of precipitation are not likely able to provide reliable precipitation quantification in the QYJ Basin at present.

In this study, we aimed to investigate the possible controls of geomorphology on precipitation in the QYJ Basin with the method of multi-year annual basin water balance. In-situ streamflow observations and an eddy flux-based evapotranspiration dataset were adopted to estimate basin annual precipitation, and in-situ precipitation of weather sites were used to reflect a spatial trend in precipitation. We first compared the differences in annual precipitation between the QYJ and adjacent basins using hydro-meteorological records, and then examined relations between the variations in precipitation and elevation. Based on precipitation comparison and transect analyses, we discussed the controls of geomorphology on the precipitation in the QYJ Basin. This study would improve our understanding about the orographic effects on precipitation and runoff production in the eastern Tibetan Plateau region.

2. Materials and Methods

2.1. Study Area

The QYJ Basin (12,600 km^2 in area) is a typical mountainous region in the eastern TP, with the elevation ranging from 500 m in the east to 4930 m in the northwest. The QYJ River is a second tributary of the upper Yangtze River, and flows into the lower Minjiang River (Figure 1). This Basin is in a horseshoe-shape with mountains at its north (>4000 m), west (~3000 m) and south (<3000 m) boundaries. The QYJ River has several tributaries, including the Yuxi River (sub-basin gauge: YX; area: 1043 km^2) and the Baoxing River (BX; 2794 km^2) in the north, the Tianquan River (TQ; 1724 km^2) and the Yingjing (YJ; 1694 km^2) in the west, the Zhougong River (KP; 1012 km^2) and the Huaxi River (TG; 698 km^2) in the south. In addition, there are two hydrological gauges on the QYJ mainstream, i.e., the DYP (1180 km^2, not including the upper sub-watersheds with gauges) and the JJ (2039 km^2). These rivers were described in Figure 1 with numbers that are explained in the figure caption. For simplicity, the gauge acronyms were used to denote corresponding sub-basins in the text. Information about these hydrological gauges was summarized in Table 1.

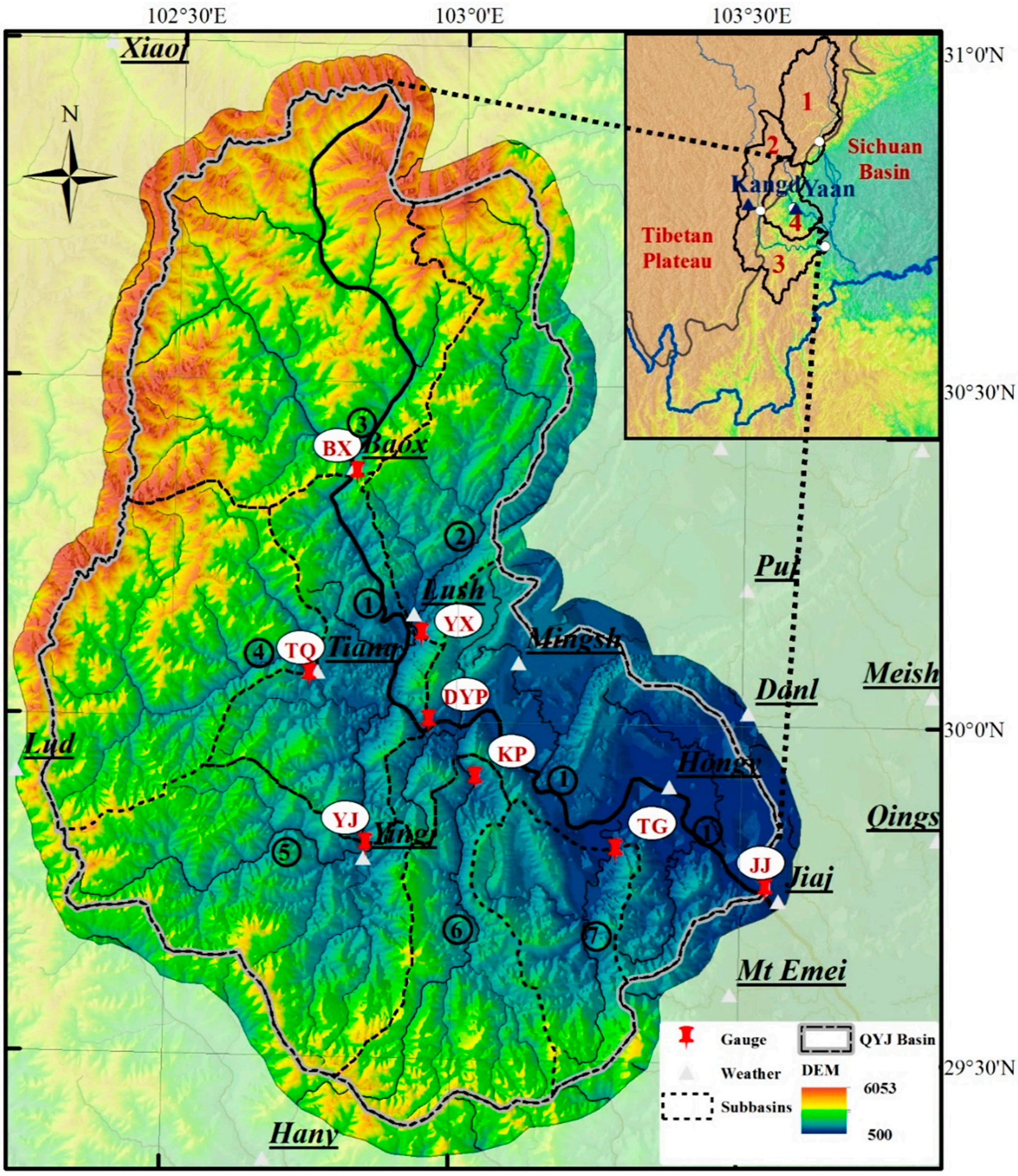

Figure 1. The geomorphology and rivers in the QYJ Basin. The numbers 1–7 in the circle respectively denote the QYJ River, Yuxi River, Baoxing River, Tianquan River, Yingjing River, Zhougong River, and Huaxi River. The labelled basins in the upright inset panel are respectively the Minjiang Basin (1, with the outlet at ZPB gauge), the middle Daduhe Basin (2, LD gauge), the lower Daduhe Basin (3, FL gauge), and the QYJ Basin (4, JJ gauge).

Table 1. The hydrological gauges in the QYJ and adjacent basins. For simplicity, the gauge names are used to denote related basins.

Basin		North		West		South		Main Stream		Adjacent		
		YX	BX	TQ	YJ	KP	TG	DYP	JJ	FL	LD	ZPB
Gauge	Lon	102.94	102.82	102.74	102.85	103.03	103.28	102.95	103.54	103.65	102.24	103.58
	Lat	30.13	30.36	30.06	29.81	29.91	29.81	30.00	29.76	29.30	29.93	31.03
Area/km^2		1365	2794	1724	1694	1012	698	1180	2039	13,600	10,114	22,662
Slope/°		23.7 ± 11.1	26.9 ± 10.6	27.7 ± 10.6	19.9 ± 10.3	18.8 ± 10.8	12.3 ± 9.4	17.1 ± 11.5	6.5 ± 8.3	22.4 ± 11.8	27.5 ± 11.5	25.0 ± 11.2
Elev/m		1939 ± 837	2986 ± 811	2435 ± 836	1802 ± 572	1770 ± 597	1232 ± 473	1270 ± 462	745 ± 266	2505 ± 1127	3811 ± 725	3340 ± 782

The "±" denotes the mean±standard deviation of slope or elevation for a certain basin.

In addition, the adjacent basins were taken to be compared with the QYJ Basin in terms of precipitation and geomorphology, including the Minjiang Basin (MJ; 22,662 km^2) above the ZPB gauge, the middle Daduhe Basin (mDDH; 10,114 km^2) above the LD gauge and the lower Daduhe Basin (lDDH; 13,600 km^2) above the FL gauge. The MJ, mDDH and lDDH basins are respectively north, west and south to the QYJ Basin, as shown in Figure 1.

2.2. Materials

In-situ records of hydro-meteorological gauges were used to describe the spatial patterns of precipitation and runoff production in the QYJ and adjacent basins. The daily streamflow records were collected at the hydrological gauges listed in Table 1. These records were mainly collected during the periods of 1965–1987 and 2007–2013. Meteorological observations of a total of 37 weather sites with and adjacent to the QYJ and neighboring basins were used to estimate site-based precipitation with the Thiessen polygon method. Especially, eight weather sites were chosen to design a latitudinal transect crossing the QYJ Basin, so as to reflect the precipitation gradient with elevation. The selected weather sites include the Rens (437 m above sea level), Qings (395 m), Hongy (463 m), Yaan (629 m), Tianq (757 m), Lud (1322 m), Kangd (2616 m), and Yaj (2599 m) in westward sequence (Figure 2b and Table 2). In addition, although local topographic features (such as aspect and slope) may have potential impacts on site-level precipitation, the regional variation in precipitation is mainly subjected to macro-geomorphology. Therefore, the study focused on the effects of macro-topographic features on precipitation instead of investigating the local features. Since major atmospheric water source of the study area is the vapor carried by the Asian Summer Monsoon from the west Pacific, annual precipitation (over 70%) occurs mainly in the summer and autumn in the form of rainfall. Therefore, snowfall is at a relatively quite low level in the study area, especially at the weather sites (below 2600 m in elevation).

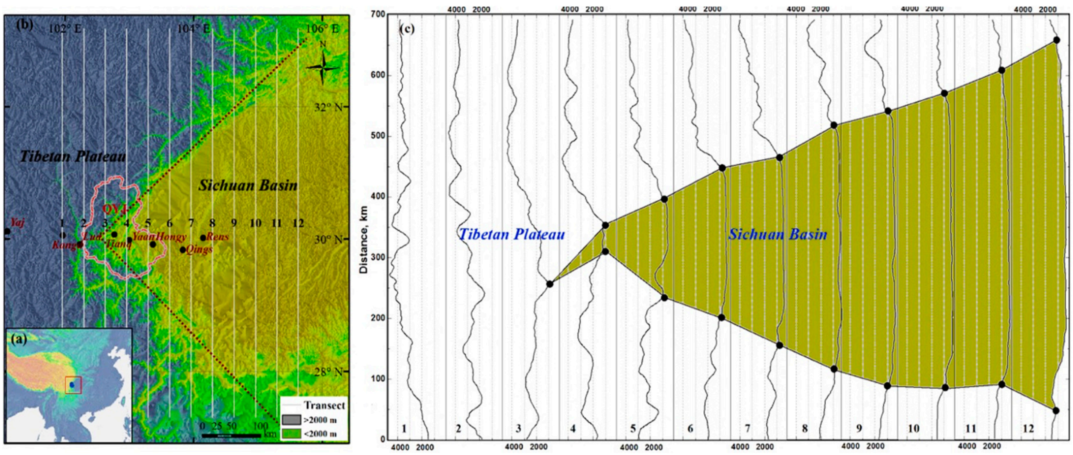

Figure 2. The location (**a**) and geomorphology (**b**) of the transition area from the Sichuan Basin to the east TP. The Sichuan Basin is embedded in the horn-mouth geomorphology of the eastern TP margin. The 12 columns in (**c**) correspond with the parallel transects in (b), and show the elevation profiles (unit: m) of these transects. The shade areas in (c) denote the west part of the Sichuan Basin.

Table 2. The weather sites of the latitudinal elevation transect crossing the study area.

Site	Rens	Qings	Hongy	Yaan	Tianq	Lud	Kangd	Yaj
Lon	30.02	29.83	29.92	29.98	30.07	29.92	30.05	30.03
Lat	104.15	103.83	103.37	103.00	102.77	102.23	101.97	101.02
Elev/m	437	395	463	629	757	1322	2616	2599

We used an evapotranspiration (ET) dataset upscaled from global FLUXNET tower observations to examine spatial variations in annual ET over the study basins [28,29]. This global half-degree flux dataset (1982–2011; noted as Jung-ET in the text) was produced by spatially upscaling FLUXNET observations with ancillary climate datasets and a satellite-based vegetation index using machine learning techniques and model tree ensembles [29]. This dataset derived annual ET (247.2 $\pm$ 55.0 mm) at a Tibetan site (92.90°E, 34.75°N, ~4600 m) that generally agreed with the in-situ lysimeter observation in 2007 and 2008 (288.4 $\pm$ 36.1 mm), indicating the favorable accuracy of this ET dataset for the TP [30]. Therefore, this ET dataset was used with streamflow observations to estimate basin-scale precipitation.

We used the satellite-based Land-cover Dataset of China (LCC-China; [31]) to examine recent land cover changes (LCC) in the study area. This dataset was produced by interpreting visual-infrared satellite images mainly acquired by the Landsat Thematic Mapper, available at a 1-km resolution for the years of 1985, 1995, 2000, 2005, and 2010 [31]. This dataset identified six major land cover classes in China (i.e., cropland, forest, grassland, water body, built-up land, and unused land) and 25 subclasses. The accuracy of six major land cover classes was reported to be above 94.3%, while the overall accuracy of 25 subclasses was above 91.2% [31]. In the study, hydrological gauge records covered the periods from 1965 to 1987 and from 2007 to 2013, so we selected the land cover maps of 1985 and 2010 to quantify LCC over of the study area during the period of 1965–2013.

2.3. Methods

This study focused on the magnitude of precipitation, so the annual scale was used in the analyses of the basin water balance. Annual precipitation of basin scale was first estimated by observations of the weather site within and adjacent to the QYJ Basin using the Thiessen polygon method (Prcp_obs). Due to sparse weather sites in the study area, we used the water balance of basin/sub-basins estimated by runoff depth and ET to reflect the spatial pattern of annual precipitation (Prcp_wb), which was an efficient means to estimate precipitation in basins with a complex terrain [25]. Runoff production and precipitation in the QYJ Basin were compared with the adjacent basins (i.e., the MJ, mDDH and lDDH basins) to distinguish precipitation characteristics. In addition, precipitation and runoff of the QYJ sub-basins were compared so as to detect their intra-basin patterns. Therefore, the streamflow of the basins and sub-basins was converted into runoff depth to make the basins comparable in terms of runoff production.

As the QYJ Basin is a part of the transition region from the Sichuan Basin (~500 m) to the eastern TP (~4000 m), a latitudinal elevation transect crossing the QYJ Basin was set to examine the variation in precipitation related to the orographic effect. This transect was over 300 km in length and included eight weather sites ranging from 395 m at the Rens to 2616 m at the Yaj in elevation (Table 2). In addition, a group of longitudinal paralleled elevation transects (totally 12 and in an interval of 40 km) were designed to examine the possible spatial pattern of macro-geomorphology on the route of ASM.

3. Results

3.1. Horn-Mouth Geomorphology

The mountain at the east TP boundary connecting with the Sichuan Basin was in a characteristic shape, i.e., a horn-mouth eastwardly facing to the source region of ASM. The QYJ Basin was at the converging point of this horn-mouth geomorphology. On the other hand, the diamond-shaped Sichuan Basin (~500 m in elevation) was embedded in this horn-mouth terrain (Figure 2). The elevation of

2000 m could well distinguish the Sichuan Basin from the surrounding mountains and plateaus, so the segments of parallel longitudinal transects falling within the Sichuan Basin reflected the width of the horn-mouth geomorphology (i.e., longitudinal width of the Sichuan Basin). The parallel longitudinal transects indicated that the width of the horn-mouth geomorphology converged from ~500 km to below 100 km over a limited latitudinal distance (320 km; Figure 2c). In such a characteristic macro-geomorphology, the terrain simultaneously lifted and narrowed from the Sichuan Basin (~500 m) to converge at the QYJ Basin (600~4500m).

3.2. Westward Variation in Precipitation

In-situ observations by weather sites on the latitudinal elevation transect showed a westward variation in precipitation (Figure 3). Spatially, annual precipitation firstly increased with the elevated terrain from 807 mm at the Rens site (437 m in elevation, ~80 km east to the QYJ Basin) to 1627 mm at the Tianq site (757 m, in the QYJ Basin), but then decreased with a further increase in elevation. Annual precipitation at the Yaj site (2616 m, ~120 km west to the QYJ Basin) was only 748 mm. Although these valley-located sites in the transition area were subjected to the influences of local specific terrains (e.g., foehn effect), their meteorological observations still reflected the strong regulation of macro-geomorphology on regional precipitation trends (site number = 5, relation = 0.788, significance level = 0.113).

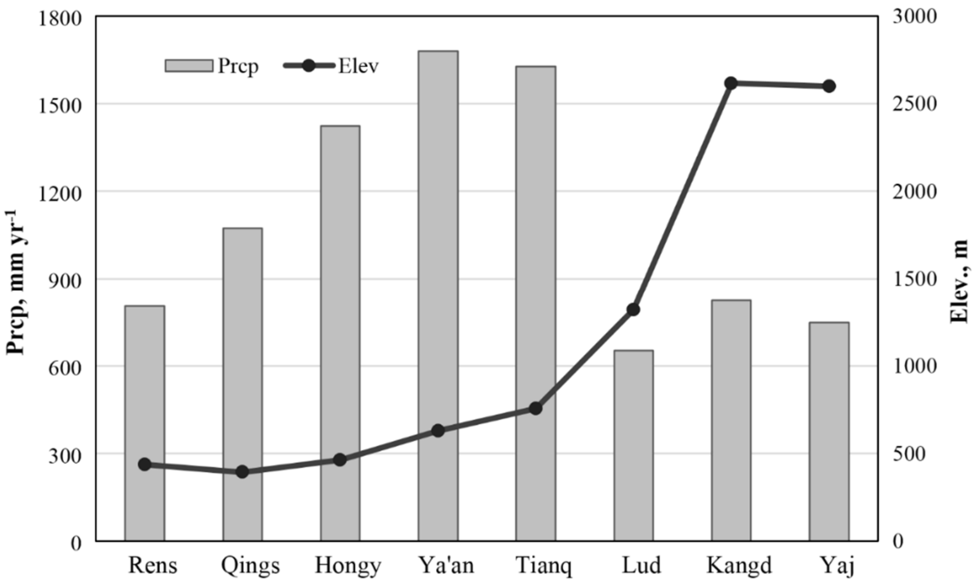

Figure 3. Variations in annual precipitation across the weather sites on the latitudinal elevation transect in the study area.

3.3. Extremely High Level of Precipitation

In-situ observations of hydrological gauges showed contrasting runoff depths between the QYJ and adjacent basins, and also contrasting between the QYJ sub-basins (Figure 4). Average annual runoff depth in the QYJ Basin was much higher (~1330 mm yr^{-1}) than the adjacent MJ Basin (667 mm yr^{-1}) and mDDH Basin (480 mm yr^{-1}) during the period of 1965–1987. However, within the QYJ Basin, runoff depth varied significantly across the sub-basins, i.e., ranging from 1034 mm yr^{-1} in the lower QYJ reach (at the JJ) to 1910 mm yr^{-1} in the middle QYJ reach (at the DYP). As the runoff depth of the rest of the QYJ sub-basins was concerned, the south sub-basin was high in annual runoff depth (averagely 1676 mm yr^{-1} in the KP and TG) while the north was low (1130 mm yr^{-1} in the YX and BX), with the temperate level in the west sub-basin (the TQ and YJ, 1452 mm yr^{-1}). In addition, the lDDH Basin also has a high annual runoff level (1370 mm yr^{-1}).

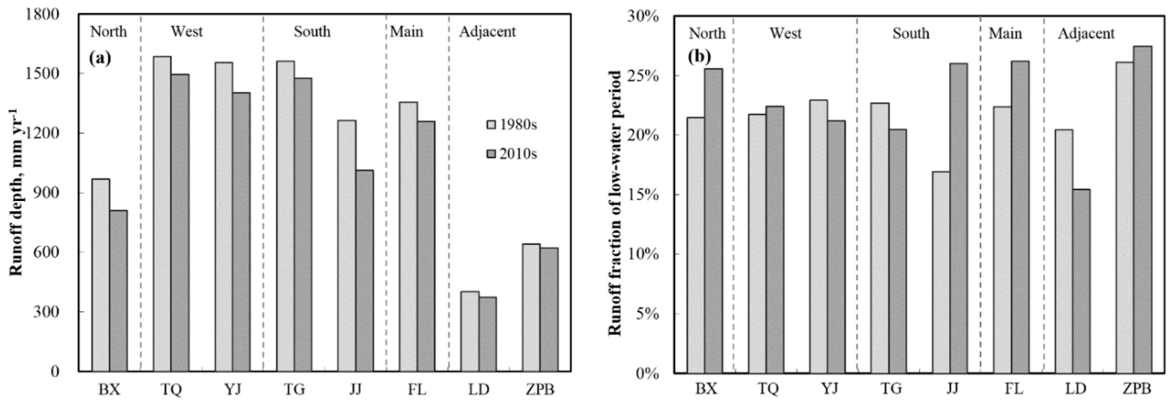

Figure 4. The changes in runoff depth during the high-flow and low-water periods (**a**) and the contribution of the low-water period (**b**) in the QYJ sub-basins and adjacent basins from the 1980s (1974–1987) to 2010s (2007–2013).

The in-situ meteorological observations (Prcp_obs) severely under-estimated the regional precipitation in both the QYJ and lDDH basins (Figure 5). In the QYJ sub-basins (except the lower reach), the annual Prcp_obs was even 100–550 mm lower than the annual runoff depth. Correspondingly, the site-based runoff coefficient (RC_obs) was surprisingly higher than 1.0, ranging from 1.08 to 1.50. Only in the lower QYJ reach (RC_obs: 0.87), MJ Basin (0.75) and mDDH Basin (0.93), were the annual Prcp_obs larger than annual runoff depth.

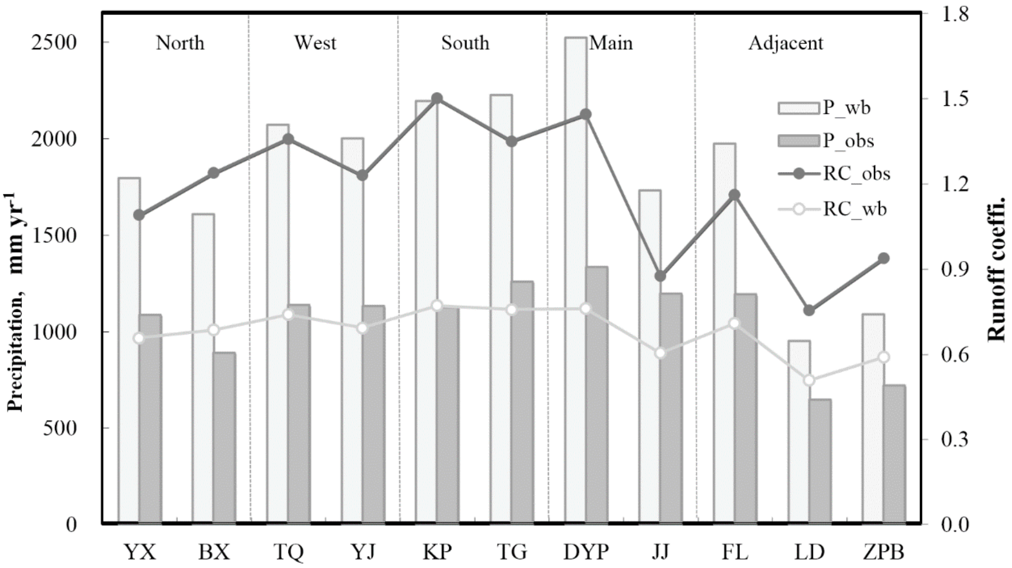

Figure 5. Spatial variations in annual basin-scale precipitation and runoff coefficient estimated respectively by water balance and weather sites in the QYJ sub-basins and adjacent basins. The hydrological gauges were used to represent corresponding basins.

The Jung-ET dataset indicated annual ET in the study basins ranging between 474 and 705 mm, with a much weaker spatial variation compared with runoff depth. Therefore, the spatial pattern of water balance-based precipitation mainly followed that of the runoff depth. Compared with the water balance-based results (Prcp_wb), the site-based observations (Prcp_obs) underestimated basin precipitation by 300–1100 mm yr^{-1} in the QYJ Basin. The annual RC (RC_wb) of the QYJ Basin based on water balance varied between 0.60 and 0.77, while those of the MJ and mDDH basins were a little lower, respectively 0.58 and 0.50 (Figure 5). However, in the lDDH Basin, the RC_wb was also relatively high (0.70) due to the high precipitation level adjacent to the horn-mouth geomorphology.

As indicated in Figure 5, the highest Prcp_wb occurred in the region with intermediate elevation, i.e., the sub-basins of KP (elevation, 1770 m; precipitation, 2196 mm yr^{-1}), TG (1232 m; 2226 mm yr^{-1}) and DYP (1270 m; 2523 mm yr^{-1}). The precipitation was a little lower (~2000 mm yr^{-1}) in the sub-basins of TQ (2435 m) and YJ (1802 m), while the sub-basins of YX and BX had the lowest Prcp_wb (respectively 1797 and 1611 mm yr^{-1}).

3.4. Decrease in Runoff Depth and ET

Records of hydrological gauges indicated a pronounced decrease in runoff production during the high-flow period (from May to October) between the two periods of 1974–1987 (1980s) and 2007–2013 (2010s) in both the QYJ and adjacent basins (Figure 4a). The runoff production during the low-water period (from November to April) also experienced a decrease in the QYJ sub-basins (Figure 4a). Therefore, all the basins had lower runoff levels of annual scale in the period of 2007–2013 than in the earlier period, especially in the QYJ (−147 mm) and lDDH (−96 mm) basins (Figure 4a).

In addition, the runoff contribution of the low-water period increased from 20.2% to 25.2% in the QYJ Basin (with internal heterogeneity) and from 22.4% to 26.2% in the lDDH Basin (Figure 4b). Meanwhile, the Jung-ET dataset reflected a slight increase in annual ET (1–12 mm) between the periods of 1982–1987 and 2007–2013 over the basins, except in the lower QYJ sub-basin (−2 mm).

4. Discussion

4.1. Controls of Geomorphology on Precipitation

The significant high level of precipitation in the QYJ Basin compared with adjacent basins could be attributed to the characteristic macro-geomorphology of the transition zone from the Sichuan Basin upward to the Tibetan Plateau. The special horn-mouth geomorphology likely had a strong converging effect on the westward atmospheric vapor transported by the Asian Monsoon. The converged air mass at the QYJ region would be further lifted by terrain from 500 m (of the Sichuan Basin) upward rapidly to over 3500 m (of the Tibetan Plateau). Therefore, the combined orographic effects of converging and lifting on the ASM vapor would lead to a high level of precipitation in the QYJ Basin (~2000 mm yr^{-1}). This was similar, though in a relatively weaker magnitude, to the case of the lower Brahmaputra valley which intercepts an extremely large magnitude of northward atmospheric vapor transported by a monsoon from the Indian Ocean [18].

The orographic effects of geomorphology on precipitation in the QYJ Basin were well-reflected by in-situ observations of the weather sites on the latitudinal elevation transect (Figure 3). Annual precipitation increased westward with the lifting relief, but then tended to decrease with a further increase in elevation. As the increasing effect of terrain-lifting on precipitation is also subjected to vapor decreasing during the lifting process, the balance between the lifting effect and the vapor decreasing determines the spatial pattern of precipitation intensity along the lifting route [14,32]. Therefore, annual precipitation generally increased with the terrain elevating till reaching the west margin of the QYJ Basin, but then began to decrease in further higher areas.

The contrast of precipitation among the QYJ and adjacent basins further indicated the significant orographic effects in the transition area between the Sichuan Basin and the eastern TP. Due to the converging and lifting effects of geomorphology on atmospheric vapor, the QYJ Basin has a high level of precipitation (~2000 mm yr^{-1}). The lDDH Basin lay immediately adjacent to the orographic converging area (Figures 1 and 2), so the annual precipitation was also at a high level (1976 mm yr^{-1}). On the contrary, as the ZPB Basin was over 100 km perpendicularly north to the vapor corridor, relatively less atmospheric vapor could be intercepted and, therefore, the precipitation level was relatively low (1092 mm yr^{-1}). Though the mDDH Basin (averagely 3811 m in elevation) was adjacent to the QYJ Basin in the west, the Prcp_wb was only 953 mm yr^{-1} possibly because the vapor magnitude had been greatly weakened before leaving the QYJ Basin.

In addition, the spatial differences of precipitation within the QYJ Basin also explained the orographic regulation of local geomorphologies on precipitation. Generally, the converged westward monsoon vapor entered the QYJ Basin from the lower QYJ valley (i.e., near the JJ gauge), and then the vapor would go upstream along valleys of the QYJ and its tributaries. As the north watersheds were distinctly higher (>4000 m) in elevation than the south (<3000 m), more monsoon vapor was possibly transported in the westward route from the JJ sub-basin to the YJ (via TG & KP) and the TQ (via DYP), as shown by Figure 1, which explained the general precipitation variations across the QYJ sub-basins. The highest Prcp_wb occurred in the region with intermediate elevation (i.e., the KP and TG sub-basin) due to the best balance between vapor magnitude and lifting effect (Figure 5). In the west sub-basins (i.e., the TQ and YJ), precipitation was a little lower because the atmospheric water vapor was gradually decreased by heavy precipitation over the eastern sub-basins (i.e., the KP and TG) promoted by the westward terrain lifting. The north sub-basins (i.e., the YX and BX) had the lowest Prcp_wb because of the blocking effect of higher mountains on vapor transporting and being relatively far (~50 km) from the converged ASM vapor.

4.2. Changes in the Water Balance

The changes in water balance in the QYJ Basin were possibly related to the expansion of forest cover during the last decades. Climate records showed little significant change in precipitation in the study area, though a warming trend of air temperature was observed during the last 45 years (~0.02 °C yr^{-1}, $p < 0.01$). The satellite-based LCC dataset indicated an increase of 7.4% in forest fraction during the period of 1985–2010, which was mainly caused by the conversions from cropland and steppe to forest (Table 3). The expansion of forest cover may restrain the runoff production due to more loss of soil water through evapotranspiration [17]. As the QYJ Basin has a rugged terrain with a slope nearly over 20° (Table 1), this Basin has relatively low levels of agricultural cultivation (17.4%) and population (420,000 in 2010 with the urban area excluded [33]). Anthropological impacts in this region were relatively low [31]. Therefore, the temporal decrease in runoff was possibly caused by more loss of soil water in the form of evapotranspiration due to forest expansion, which was consistent with the slight increase in annual ET reflected by the Jung-ET dataset. This fact implied that the increase in forest fraction may help to mitigate the flood threat by reducing surface runoff in this pluvial basin.

Table 3. Land cover changes in the QYJ Basin from 1985 to 2010 (km^2).

Change	Forest	Steppe	Cropland	Urban
Increase	967.5	217.1	81.2	8.9
Decrease	57.7	402.3	714.6	0.0
Net increase	909.8	−185.2	−733.5	8.9

4.3. Uncertainties in the Precipitation Estimation

In the study, the orographic effect of geomorphology on precipitation was investigated using the water balance method (Prcp_wb). The possible uncertainties in the Prcp_wb estimation may result from the ET dataset and the changes in terrestrial water storage. The ET in the study was estimated with the half-degree Jung-ET dataset, which was validated at one site with lysimeter observation [30]. The estimated annual ET varied between 470 mm and 710 mm across the study basins, and was a relatively small component of water balance compared with the annual runoff depth in the QYJ Basin (>1100 mm). So the ET-caused uncertainty in the Prcp_wb estimation was limited.

In addition, there were no glaciers, intensive groundwater-withdrawal and large reservoirs in the QYJ Basin [6], and the changes in annual water storage were possibly very low. We investigated the precipitation regime of the study area based on a multi-year average water balance (~10 years), and therefore the decadal variation in basin water storage would be very weak. A basin-scale diagnostic dataset of monthly variations in terrestrial water storage of large river basins (BSWB v2016) was taken to examine the multi-year balance of the Yangtze River Basin above Yichang gauge, where the QYJ Basin was included. This dataset was produced based on atmospheric and terrestrial water balances with streamflow measurements and reanalysis atmospheric moisture [34,35]. This dataset indicated that the Yangtze River Basin was relatively weak in annual variation during the period of 1979–1986 (multi-year averagely below 1.0 mm yr^{-1}). Therefore, the uncertainties in basin-scale precipitation estimated by water balance likely had only slight influences on the analysis of orographic effects in the study.

5. Conclusions

In the study, we investigated the orographic effects of geomorphology on precipitation in a typical pluvial basin with in-situ streamflow observations and an eddy flux-based ET dataset. Our results showed that site-observed annual precipitation (~1150 mm yr^{-1}) was much lower than basin runoff depth (~1450 mm yr^{-1}) in the QYJ Basin. Water balance indicated a much higher precipitation level (averagely ~2000 mm yr^{-1}) in the QYJ Basin, but the precipitation was quite low in two adjacent regions (<1000 mm yr^{-1}). The spatial pattern of precipitation was well consistent with the horn-mouth shape of the eastern TP margin, with more precipitation occurring in the geomorphological converging region (i.e., the QYJ Basin). In addition, the increase in forest fraction (7.4%) from the 1980s to 2010s possibly resulted in the decrease in runoff production (~133 mm yr^{-1}). With this study, we could conclude that the high level of precipitation and its spatial heterogeneity in the QYJ Basin could be attributed to the combined converging and lifting effects of geomorphology on the westward atmospheric vapor from the western Pacific. The understanding regarding the orographic effects on precipitation and runoff production could be considered in the water resource management and flood mitigation in the eastern Tibetan Plateau.

Author Contributions: Conceptualization, M.Y. and W.Z.; Methodology, M.Y. and W.Z.; Writing-Original Draft Preparation, M.Y.; Writing-Review & Editing, M.Y. and W.Z.

Acknowledgments: This work was supported by the National Natural Science Foundation of China (41771112) and the Natural Science Foundation of Shanxi Province, China(201801D121266).

Conflicts of Interest: The authors declare no conflict of interest.

References

1. Wu, G.; Duan, A.; Liu, Y.; Mao, J.; Ren, R.; Bao, Q.; He, B.; Liu, B.; Hu, W. Tibetan Plateau climate dynamics: Recent research progress and outlook. *Natl. Sci. Rev.* **2015**, *2*, 100–116. [CrossRef]
2. Zheng, D. *The Zoning of Ecographical Systems in China*; The Commercial Press: Beijing, China, 2008. (In Chinese)
3. Dahri, Z.H.; Ludwig, F.; Moors, E.; Ahmad, B.; Khan, A.; Kabat, P. An appraisal of precipitation distribution in the high-altitude catchments of the Indus basin. *Sci. Total Environ.* **2016**, *548–549*, 289–306. [CrossRef] [PubMed]
4. Kang, S.; Xu, Y.; You, Q.; Flügel, W.-A.; Pepin, N.; Yao, T. Review of climate and cryospheric change in the Tibetan Plateau. *Environ. Res. Lett.* **2010**, *5*, 015101. [CrossRef]
5. Yao, T.; Masson-Delmotte, V.; Gao, J.; Yu, W.; Yang, X.; Risi, C.; Sturm, C.; Werner, M.; Zhao, H.; He, Y.; et al. A review of climatic controls on $\delta^{18}O$ in precipitation over the Tibetan Plateau: Observations and simulations. *Rev. Geophys.* **2013**, 51. [CrossRef]
6. Zhang, L.; Su, F.; Yang, D.; Hao, Z.; Tong, K. Discharge regime and simulation for the upstream of major rivers over Tibetan Plateau. *J. Geophys. Res. Atmos.* **2013**, *118*, 8500–8518. [CrossRef]
7. Huang, Y.; Cui, X. Moisture sources of an extreme precipitation event in Sichuan, China, based on the Lagrangian method. *Atmos. Sci. Lett.* **2015**, *16*, 177–183. [CrossRef]
8. Li, Q.; Yang, G. Temporal distribution characteristics of alpine precipitation and their vertical differentiation: A case study from the upper Shule River. *Water* **2017**, *9*, 284. [CrossRef]
9. Smith, R.B.; Jiang, Q.; Fearon, M.G.; Tabary, P.; Dorninger, M.; Doyle, J.D.; Benoit, R. Orographic precipitation and air mass transformation: An alpine example. *Q. J. R. Meteorol. Soc.* **2003**, *129*, 433–454. [CrossRef]

10. Wu, C.-H.; Chou, M.-D. Tibetan Plateau westerly forcing on the cloud amount over Sichuan Basin and the early Asian summer monsoon. *J. Geophys. Res. Atmos.* **2013**, *118*, 7558–7568. [CrossRef]
11. Zangl, G. Small-scale variability of orographic precipitation in the Alps: Case studies and semi-idealized numerical simulations. *Q. J. R. Meteorol. Soc.* **2007**, *133*, 1701–1716. [CrossRef]
12. Zeng, W.; Yu, Z.; Wu, S.; Qin, J. Changes in annual, seasonal and monthly precipitation events and their link with elevation in Sichuan province, China. *Int. J. Climatol.* **2016**, *36*, 2303–2322. [CrossRef]
13. Rotunno, R.; Houze, R.A. Lessons on orographic precipitation from the Mesoscale Alpine Programme. *Q. J. R. Meteorol. Soc.* **2007**, *133*, 811–830. [CrossRef]
14. Jiang, Q. Moist dynamics and orographic precipitation. *Tellus A* **2003**, *55*, 301–316. [CrossRef]
15. Jiang, Q. Precipitation over multiscale terrain. *Tellus A* **2007**, *59*, 321–335. [CrossRef]
16. Roe, G.H.; Montgomery, D.R.; Hallet, B. Orographic precipitation and the relief of mountain ranges. *J. Geophys. Res. Solid Earth* **2003**, 108. [CrossRef]
17. Zhang, K.; Pan, S.; Cao, L.; Wang, Y.; Zhao, Y.; Zhang, W. Spatial distribution and temporal trends in precipitation extremes over the Hengduan Mountains region, China, from 1961 to 2012. *Quat. Int.* **2014**, *349*, 346–356. [CrossRef]
18. Andermann, C.; Bonnet, S.; Gloaguen, R. Evaluation of precipitation data sets along the Himalayan front. *Geochem. Geophys. Geosyst.* **2011**, 12. [CrossRef]
19. Liu, M.; Xu, X.; Sun, A. Decreasing spatial variability in precipitation extremes in southwestern China and the local/large-scale influencing factors. *J. Geophys. Res. Atmos.* **2015**, *120*, 6480–6488. [CrossRef]
20. Yang, K.; Ye, B.; Zhou, D.; Wu, B.; Foken, T.; Qin, J.; Zhou, Z. Response of hydrological cycle to recent climate changes in the Tibetan Plateau. *Clim. Chang.* **2011**, *109*, 517–534. [CrossRef]
21. Breña-Naranjo, J.A.; Pedrozo-Acuña, A.; Rico-Ramirez, M.A. World's greatest rainfall intensities observed by satellites. *Atmos. Sci. Lett.* **2015**, *16*, 420–424. [CrossRef]
22. Mahanta, R.; Sarma, D.; Choudhury, A. Heavy rainfall occurrences in northeast India. *Int. J. Climatol.* **2013**, *33*, 1456–1469. [CrossRef]
23. Shu, S.-J.; Yu, Z.-F.; Wang, Y.; Bai, M. A statistic model for the spatial distribution of precipitation estimation over the Tibetan complex terrain. *Chin. J. Geophys.* **2005**, *48*, 593–601. [CrossRef]
24. Hu, L.; Deng, D.; Gao, S.; Xu, X. The seasonal variation of Tibetan convective systems: Satellite observation. *J. Geophys. Res. Atmos.* **2016**, *121*, 5512–5525. [CrossRef]
25. Henn, B.; Clark, M.P.; Kavetski, D.; Newman, A.J.; Hughes, M.; McGurk, B.; Lundquist, J.D. Spatiotemporal patterns of precipitation inferred from streamflow observations across the Sierra Nevada mountain range. *J. Hydrol.* **2018**, *556*, 993–1012. [CrossRef]
26. Tong, K.; Su, F.; Yang, D.; Zhang, L.; Hao, Z. Tibetan Plateau precipitation as depicted by gauge observations, reanalyses and satellite retrievals. *Int. J. Climatol.* **2014**, *34*, 265–285. [CrossRef]
27. Zhao, T.; Yatagai, A. Evaluation of TRMM 3B42 product using a new gauge-based analysis of daily precipitation over China. *Int. J. Climatol.* **2014**, *34*, 2749–2762. [CrossRef]
28. Baldocchi, D.; Falge, E.; Gu, L.; Olson, R.; Hollinger, D.; Running, S.N.; Anthoni, P.; Bernhofer, C.; Davis, K.; Evans, R.; et al. Fluxnet: A new tool to study the temporal and spatial variability of ecosystem-scale carbon dioxide, water vapor, and energy flux densities. *Am. Meteorol. Soc. Bull.* **2001**, *82*, 2415–2434. [CrossRef]
29. Jung, M.; Reichstein, M.; Margolis, H.A.; Cescatti, A.; Richardson, A.D.; Arain, M.A.; Arneth, A.; Bernhofer, C.; Bonal, D.; Chen, J.; et al. Global patterns of land-atmosphere fluxes of carbon dioxide, latent heat, and sensible heat derived from eddy covariance, satellite, and meteorological observations. *J. Geophys. Res. Biogeosci.* **2011**, 116. [CrossRef]
30. Fan, X. *Influence of Vegetation Coverage on Evapotranspiration Procees of Alpine Meadows in the Source Region of Yangtze River*; Lanzhou University: Lanzhou, China, 2011.
31. Liu, J.; Kuang, W.; Zhang, Z.; Xu, X.; Qin, Y.; Ning, J.; Zhou, W.; Zhang, S.; Li, R.; Yan, C.; et al. Spatiotemporal characteristics, patterns, and causes of land-use changes in China since the late 1980s. *J. Geogr. Sci.* **2014**, *24*, 195–210. [CrossRef]
32. Barstad, I.; Grabowski, W.W.; Smolarkiewicz, P.K. Characteristics of large-scale orographic precipitation: Evaluation of linear model in idealized problems. *J. Hydrol.* **2007**, *340*, 78–90. [CrossRef]
33. Sichuan, S.B. *Sichuan Statistical Yearbook*; China Statistics Press: Chengdu, China, 2017.

34. Hirschi, M.; Seneviratne, S.I. Basin-scale water-balance dataset (BSWB): An update. *Earth Syst. Sci. Data* **2017**, *9*, 251–258. [CrossRef]
35. Hirschi, M.; Seneviratne, S.I.; Schär, C. Seasonal variations in terrestrial water storage for major midlatitude river basins. *J. Hydrometeorol.* **2006**, *7*, 39–60. [CrossRef]